Photodissociation of Nitrosobenzene (C_6H_5NO) at 266 nm

Jian-Hua Huang, Guang-Jun Wang, Xi-Bin Gu, Ke-Li Han,* and Guo-Zhong He

State Key Laboratory of Molecular Reaction Dynamics, Dalian Institute of Chemical Physics, Chinese Academy of Sciences, Dalian 116023, China

Received: October 1, 1999; In Final Form: July 26, 2000

The ultraviolet photodissociation of nitrosobenzene at 266 nm has been performed on a universal crossed molecular beams machine with a TOFMS detector. The time-of-flight spectra of the NO and C_6H_5 photofragments have been measured. The TOF spectra evidence only one component. The measured photofragment translational energy distribution $P(E_t)$ reveals that about 29% of the available energy is partitioned into translational energy. The anisotropy parameter β at this wavelength is −0.64. From $P(E_t)$ and β, we deduce that during the photodissociation of C_6H_5NO, a perpendicular transition dominates over a parallel transition. Ab initio calculations were also performed to interpret the mechanism of the photodissociation.

1. Introduction

The investigation of the photodissociation of polyatomic molecules is a profitable step toward the understanding of the microscopic dynamics of chemical reactions.[1,2] Photofragment translational spectroscopy (PTS)[3−7] has provided an ideal tool for investigating photodissociation dynamics in a collision-free regime. From these experiments, we can obtain the product states, branching ratios, fragment translational energy distributions, and angular distributions of the photofragments. Thus, we can understand the energy distribution relationship between translational and internal energies. Furthermore, information about photodissociation processes such as the dissociative lifetime of the parent molecule, the orientation of the transition dipole moment, and the symmetry change of the highly excited states can also be deduced from the experimental results.

Recently, photodissociation of a series of aryl halides and alkyl halides[8−13] was performed in our group using PTS. Several other groups[14−22] had also reported the results of photodissociation for the aryl halides. The general viewpoint about the dissociation mechanism is that aryl halides are predissociated, in contrast to the direct dissociation of alkyl halides. Some alkyl halides such as CH_3Cl,[23,24] CH_3Br,[25] CH_3I,[26−28] and CH_2BrI[29,30] have well been investigated by photofragment translational spectroscopy, and the results reveal that these molecules undergo fast photodissociation by a transition to the repulsive (n,σ*) state, leading to direct dissociation with a concomitant large translational energy release.

Instead of detecting an atom fragment, detection of the diatomic fragment is also interesting because diatomic photofragments can be analyzed with TOFMS, LIF, or both. Nitroso compounds (R−NO) seem to be good candidates for such studies. For instance, experimental studies of the 450−700 nm photodissociation dynamics of NCNO,[31−33] $(CH_3)_3CNO$,[34,35] HNO,[36] CF_3NO,[37−44] and CF_2ClNO[45] have been conducted by photofragment translational spectroscopy (PTS) or by monitoring the nascent NO product using the one- or two-photon laser-induced fluorescence technique. A general picture of the gas-phase photofragmentation mechanism of nitrosoalkanes has emerged. In this wavelength range, the absorption is assigned to the $S_1{}^1A'' \leftarrow S_0{}^1A'$ transition. The $S_1{}^1A''$ state has a high energy barrier to C−N bond dissociation, and fragmentation occurs on the $S_0{}^1A'$ and $T_1{}^3A''$ surfaces following intramolecular vibrational energy redistribution and nonradiative electronic relaxation. Only a few experimental and theoretical studies have hitherto been carried out on the ultraviolet absorption spectrum of nitrosobenzene.[46−48] This might be due to the fact that nitrosobenzene is rather unstable and its ultraviolet absorption spectrum too complicated to be understood by analogy with that of benzene. Tabei et al.[48] indicated that nitrosobenzene exhibited five absorption maxima in the ultraviolet region at 301.4, 280.5, 218, 194, and 174 nm. The two shorter-wavelength bands (174 and 194 nm) may be regarded as the shifted $A_{1g} \rightarrow E_{1u}$ and $A_{1g} \rightarrow B_{1u}$ bands of benzene. The 218 nm band corresponds mainly to the $A_{1g} \rightarrow B_{2u}$ band of benzene. The 280.5 nm band can be regarded as the charge-transfer absorption band, which is caused by an electron transfer from the benzene ring to the nitroso group, and the 301.4 nm transition may correspond to mixed excitation within the benzene ring and the charge-transfer excitation.

Nitro and nitroso compounds are interesting species because of their relevance to combustion and to the decomposition of energetic materials[49−51] and because of their potential role in atmospheric chemistry.[52,53] Galloway and co-workers[54] reported their results on the photolysis of nitrobenzene at wavelengths between 220 and 320 nm and obtained the primary dissociation pathways and kinetic energy disposal by vacuum-ultraviolet-photoionization time-of-flight (TOF) mass spectrometric product identification. The rate constant for the unimolecular decomposition of nitrosobenzene was first measured with Choo et al.'s[55] very low-pressure pyrolysis method, which provided the widely accepted C−N bond dissociation energy $D(C_6H_5-NO) = 51 \pm 1$ kcal/mol. More recently, the unimolecular decomposition of C_6H_5NO was studied by Lin et al.,[56] who used the pyrolysis-FTIR spectrometric method, and they obtained the high-pressure thermal decomposition rate constant and the C−N bond strength. However, there are no reports on the photodissociation dynamics of nitrosobenzene at any wavelength. In this paper, the experimental results of C_6H_5NO photodissociation at 266 nm are first reported. The photodissociation mechanisms of nitrosobenzene are also discussed. In addition, we report the geometries of the electronic ground state and some excited states optimized by means of an ab initio method in order to explain the dissociation mechanism.

* Corrresponding author.

10.1021/jp993526i CCC: $19.00
Published on Web 10/05/2000

2. Experimental Procedures

The universal crossed molecular beams machine for the present experiment has been described in detail elsewhere.[57] This machine can be used to investigate both reactive scattering[58] and photodissociation dynamics.[8−13] In the latter case, a supersonic molecular beam is replaced by a laser beam. Briefly, a differentially pumped molecular beam is crossed at a right angle with a laser beam in the main chamber, and the photofragments are ionized in a Brinks electron bombardment ionizer, analyzed by a quadrupole mass filter, and then detected by a Daly-type ion counter consisting of a 30 kV ion target, a scintillator, and a photomultiplier. The signals are preamplified, discriminated, and then registered with a 4096 channel multichannel scalar (MCS) installed in a Pentium PC. The detector is triply pumped with three ion pumps and can be rotated in plane from −8° to 110° with respect to the source molecular beam. The flight path from the interaction region to the center of the electron impact ionizer is 19 cm, and most of our data have been recorded with a dwell time of 2 μs per channel. During the experiment, the pressures in the main chamber and the ionizer region are kept under 8×10^{-4} and 2×10^{-7} Pa, respectively. The supersonic molecular beam is prepared by seeding nitrosobenzene in helium and expanding the mixture into the source chamber through a 0.20 mm nozzle. Because nitrosobenzene is solid (mp, 67−69 °C) at room temperature, we heated it to about 69 °C during the experiment (seed ratio, ~4%). The beam velocity distribution measurements are performed by chopping the beam with a spinning disk with one slit (about 0.1 cm). The molecular source beam TOF measurement is fitted with the program KELVIN[59] to an assumed form for the velocity distribution,[60] $N(v) \propto v^2 \exp[-(v/\alpha - S)^2]$. α and S in this work are determined to be 473.6 m/s and 2.151 cm/s, respectively.

The 266 nm output of a Nd:YAG laser is focused to a 5.0 mm^2 spot at the intersection of the laser and molecular beams. The laser is operated at a repetition rate of 10 Hz. The laser pulse energy is typically 40 mJ. Nitrosobenzene (Fluka, >99%) is obtained commercially and is used without further purification. TOF measurements are made at different detector angles.

3. Results and Analysis

The angle-resolved TOF spectra detected at $m/e = 30$ corresponding to NO at 10°, 15°, 17.5°, and 20° relative to the molecular beam are shown in Figure 1. The TOF spectra detected at $m/e = 77$ corresponding to C_6H_5 are shown in Figure 2. The TOF spectra evidence one component attributed to photodissociation via single-photon absorption. The power-dependence measurements have been carefully conducted, and for the best signal-to-noise ratio, we choose the current laser power. The background has been subtracted from all spectra in Figures 1 and 2.

The solid lines in Figures 1 and 2 represent the calculated TOF spectra obtained via the forward convolution method.[61,62] The essence of the forward convolution method is to fit TOF spectra at different angles and angular distributions simultaneously through iterative adjustment of the total center-of-mass (CM) translational energy distribution and angular distribution $w(\theta)$. The angular distribution takes the form[63]

$$w(\theta) = \frac{1}{4\pi}[1 + \beta P_2(\cos\theta)] \qquad (1)$$

in which P_2 is the second-order Legendre polynomial, θ is the angle between the electric vector of laser field and the recoiling

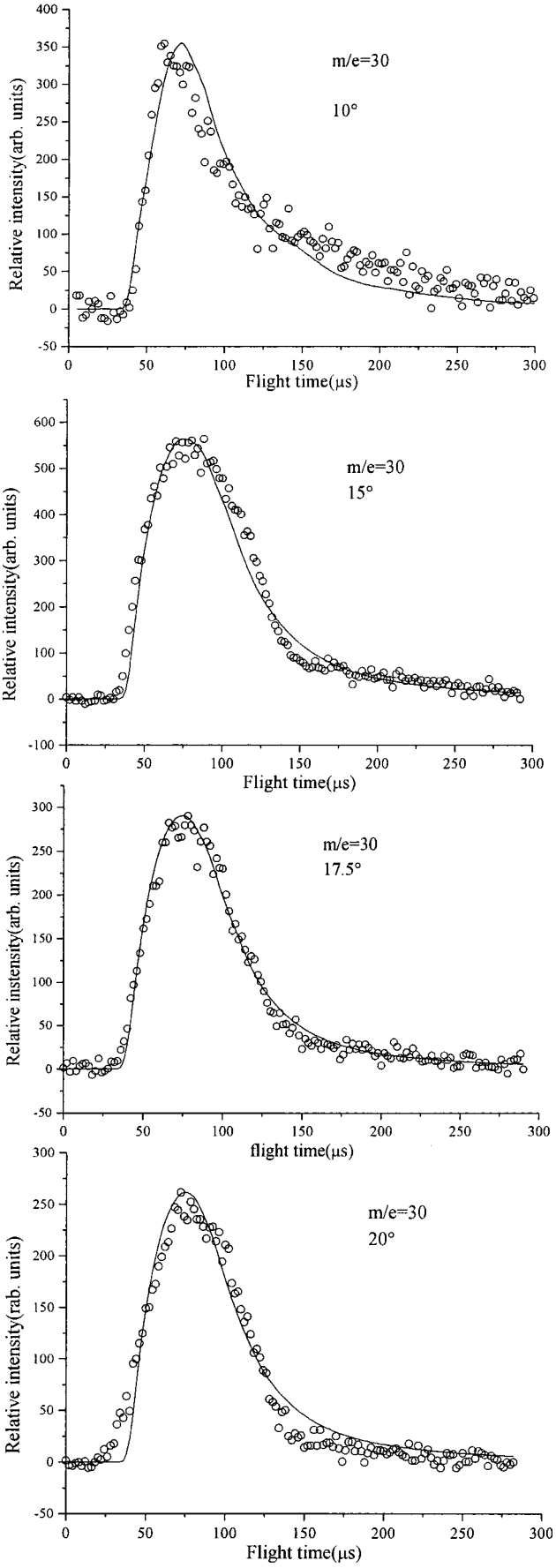

Figure 1. Laboratory TOF distribution of NO ($m/e = 30$) fragments at detector-to-source angles of 10°, 15°, 17.5°, and 20°: (○) experimental points, (—) best fitting by using $\beta = -0.64$ and the total translational energy $P(E_t)$ shown in Figure 3.

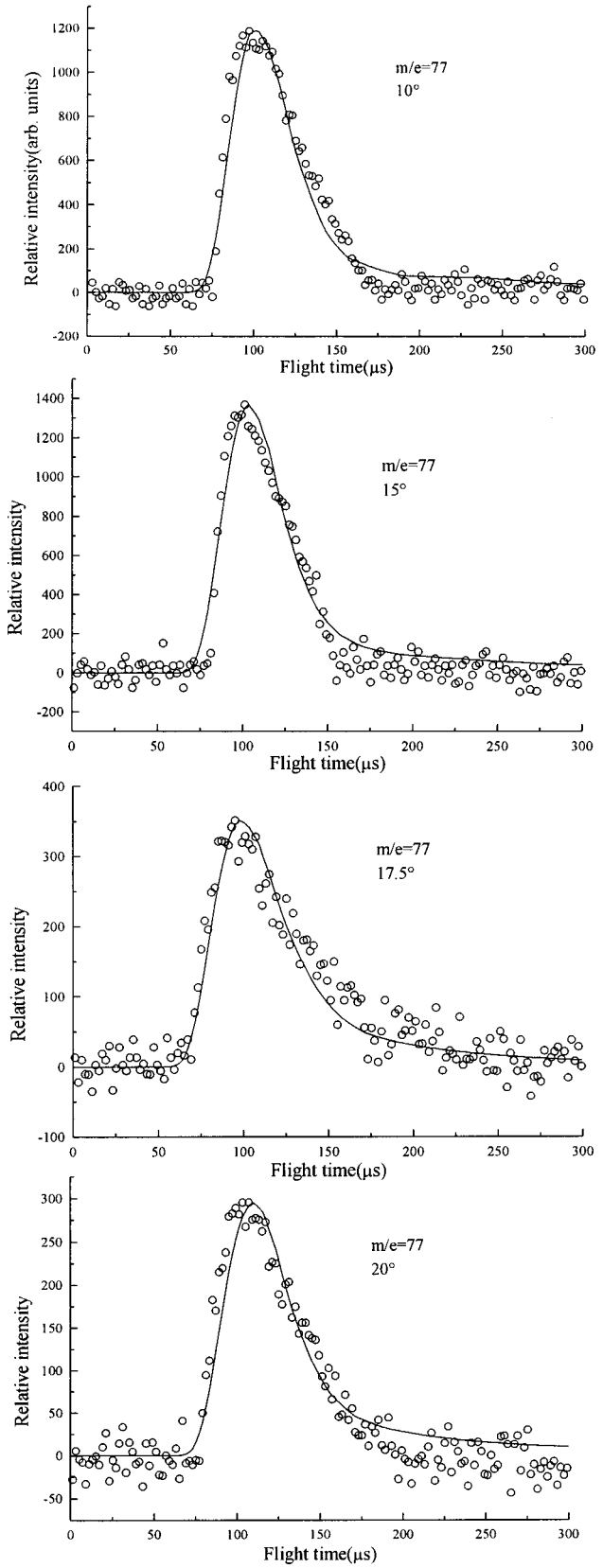

Figure 2. Laboratory TOF distribution of C_6H_5 ($m/e = 77$) fragments at detector-to-source angles of 10°, 15°, 17.5°, and 20°: (○) experimental points, (—) best fitting by using $\beta = -0.64$ and the total translational energy $P(E_t)$ shown in Figure 3.

direction of photofragments in the CM frame, and β is the anisotropy parameter whose range is from −1 to 2.

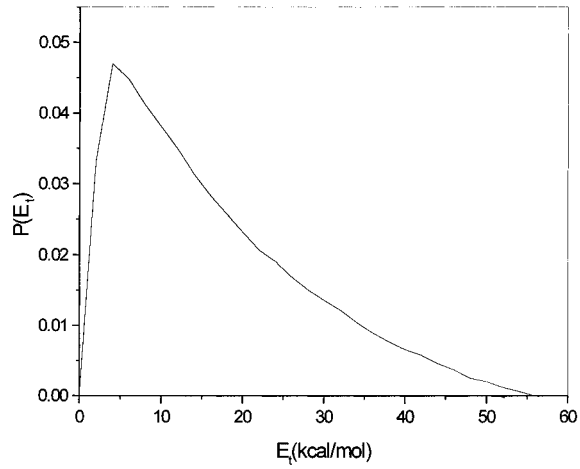

Figure 3. Total center-of-mass translational energy distribution in the photodissociation of nitrosobenzene at 266 nm.

Via the forward convolution fitting, we arrive at the CM total translational energy distribution $P(E_t)$, shown in Figure 3. It has an average translational energy $\langle E_t \rangle$ of 16.25 kcal/mol. The translational energy distribution is relatively wide, with the probability extending to about 55 kcal/mol. The available energy is given by

$$E_{avl} = h\nu + W_{int} - D_0(C-N) = E_t + E_{int} \qquad (2)$$

where $h\nu$ is the photon energy (107.5 kcal/mol for 266 nm) and D_0 is the dissociation energy. W_{int} is the internal energy of the parent molecule, which can be neglected since a supersonic molecular beam is employed in our experiment. E_{int} denotes the internal energies of the fragments. From $P(E_t)$, we can estimate the dissociation energy D_0 to be ∼52.5 kcal/mol, which is very close to the widely accepted C−N bond dissociation energy $D(C_6H_5-NO) = 51 \pm 1$ kcal/mol.[55] From eq 2, we can deduce the energy distribution relationship between translation and internal energy excitation. For C_6H_5NO photodissociation at 266 nm, about 29% of the available energy (16.25 kcal/mol) is partitioned into translational energy and about 71% (40.25 kcal/mol) into internal excitation.

The best-fit anisotropy parameter β is -0.64 ± 0.1, derived from the forward convolution method. According to Bersohn's pseudodiatomic model,[16] β can be related to the orientation of transition dipole moment and the dissociative lifetime through

$$\beta = yP_2(\cos\chi) \qquad (3)$$

where P_2 denotes the second-order Legendre polynomial, χ is the angle between the electric transition dipole moment and the recoiling direction, and y is a factor related to the lifetime of the dissociative state. This factor assumes a maximum value of 2 in the limit of instantaneous dissociation and decreases monotonically with increasing lifetime. From the β value, we cannot simultaneously determine the dissociative lifetime and χ value, but we can determine the range of χ values. If β is positive, the direction of dissociation makes an angle $\chi < 54.7°$ with respect to the transition dipole moment, and if β is negative, the direction of dissociation makes an angle $\chi > 54.7°$. Two extreme situations are $\beta = 2$ and $\beta = -1$, corresponding to $\chi = 0°$ (parallel transition) and $\chi = 90°$ (perpendicular transition), respectively. In our case, $\beta = -0.64 \pm 0.1$, which indicates that a perpendicular transition plays a central role in nitrosobenzene photolysis at 266 nm.

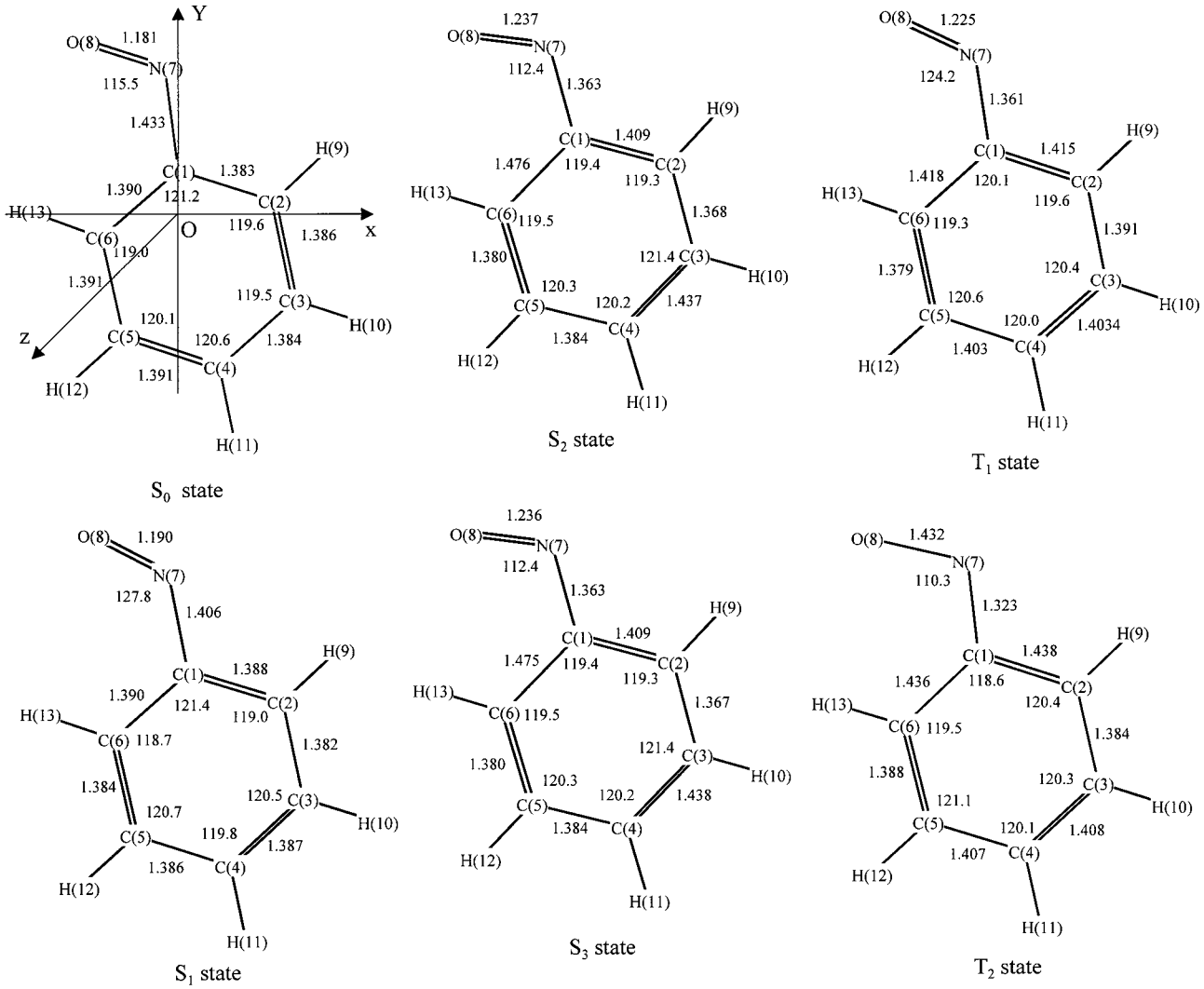

Figure 4. Geometries of C_6H_5NO calculated by using the GAUSSIAN 94 package. The ground state (S_0) is optimized at the HF/6-31G** level; the first (S_1) and the second (S_2) singlet excited states are at the CIS/6-31G** level; the first (T_1) and the second (T_2) triplet excited states are at the UHF/6-31G** level.

4. Discussion

Photodissociation dynamics of some nitroso alkyl and its derivatives[31−45] shows that in this wavelength range the absorption is assigned to a $S_1{}^1A'' \leftarrow S_0{}^1A'$ ($n-\pi^*$) transition; because the $S_1{}^1A''$ state has high energy barrier to C−N bond dissociation, fragmentation might occur on the $S_0{}^1A'$ and $T_1{}^3A''$ surfaces following intramolecular vibrational energy redistribution and nonradiative electronic relaxation. However, there also exist different mechanisms—for instance, $(CH_3)_2NNO$[64] photodissociation—that show a large fraction of the available energy is converted into the translational motion of the fragments; this result is characteristic of a direct dissociation mechanism on a repulsive S_1 potential surface. This dissociation behavior leads to a rotational and vibrational energy distribution in NO, which strongly differs from a statistical distribution. The findings are qualitatively very similar to those reported for CH_3ONO.[65] However, only 29% of the available energy is partitioned into translational energy in our experiment, indicating that the dissociation mechanism may be different. In reports of the photodissociation of NCNO by Pfab and co-workers,[66] the primary dissociation step can consist either of predissociation by internal conversion to the X^1A' continuum or of intersystem crossing to a bound or repulsive $^3A''$ state. They did not find spectroscopic evidence in absorption for this elusive triplet state in the near-infrared region. They prefer the first mechanism and, in analogy, the internal conversion consisting of the transfer of bound states of $^1A''$ to the continuum of the ground-state parent molecule. The mechanism of CF_3NO dissociation has been the subject of much previous work. The general view is that the NO fragment arises from the predissociation of the S_1 state of CF_3NO involving S_0 or T_1 as intermediates. Very recently, Cline et al.[44] studied the CF_3NO photodissociation in more detail. Measurements of photoproduct recoil-speed distributions of the NO fragment at 585 nm are bimodal, with the higher-speed component attributed to dissociation across a potential barrier on the T_1 surface and the lower-speed component attributed to dissociation on the S_0 surface.

The absorption spectrum of nitrosobenzene is relatively complicated, according to the calculation of Tabei and Nagakura.[48] The 266 nm excitation wavelength lies on the blue side of the 280.5 nm band, assigned to a charge-transfer absorption band caused by an electron transfer from the benzene ring to the nitroso group, which might be a ($\pi-\pi^*$) transition. However, Testa[67] believed that although no distinct n,π^* absorption band in the UV has been assigned to nitrosobenzene, it was probably buried under the long-wavelength side of the strong absorption appearing at about 308 nm. To better illustrate the possible dissociation mechanism, we performed ab initio

TABLE 1: Calculation Results Using the GAUSSIAN 94 Package[a]

		TEDM[b]			
	ΔE[c] (nm)	*X*	*Y*	*Z*	osc.[d]
$S_0 \rightarrow S_1$	789.92	0.0000	0.0000	−0.1497	0.0009
$S_0 \rightarrow S_2$	213.12	0.3235	0.6259	0.0000	0.0707

[a] It is clear that the transition energy of S_1 is less than the photon energy; however, the transition energy of S_2 is greater than its photon energy. The direction of the $S_0 \rightarrow S_1$ transition is along the *Z* coordinate axis, and the $S_0 \rightarrow S_2$ transition is in the *XY* plane. According to the anisotropy parameter β and the transition energies, the electronic transition at 266 nm should be the $S_0 \rightarrow S_2$ transition. [b] Transition electronic dipole moment in standard orientation (shown in Figure 4). [c] Transitional energy from the ground state to the excited state. [d] Oscillator strength.

calculations for the electronic ground state (S_0), the first (S_1) and the second (S_2) excited singlet states, and the first (T_1) and the second (T_2) excited triplet states using the Gaussian 94 electronic structure package.[68] In the electronic ground state, geometry optimization is performed at the HF/6-31G** level. For the calculation of the excited singlet states, the Hartree−Fock CI Singles (CIS) approach[69,70] is used, in which the excited-state wave function is expanded in the set of singly excited Slater determinants generated by promoting one electron from an occupied orbital to a virtual orbital. The geometries of the triplet excited states are optimized at the UHF/6-31G** level. The optimized geometries in standard orientation are shown in Figure 4. The standard orientation is that the origin of coordinate is at the CM of the molecule, and the coordinate axes are the three principal axes of inertia. Generally, the geometries of excited states are different from that of the ground state: the C−C bond lengths of the benzene ring increase slightly for the excited state. The electronic transition dipole moments in standard orientation from the ground state to the S_1 and S_2 states are presented in Table 1. Clearly, both transition dipole moments are preferentially perpendicular to the line from the CM of NO to the CM of C_6H_5. This implies that the transitions of experimental observation may be either $S_0 \rightarrow S_1$ or $S_0 \rightarrow S_2$ since the experimental β value is negative. The excited energies for the first and the second excited singlet states are 2.0194 eV (789.92 nm) and 4.9594 eV (213.12 nm), respectively. The calculated vertical excitation energy to the S_2 state is a little higher than the photon energy, whereas the calculated vertical excitation energy to the S_1 state greatly deviates from 266 nm. This may indicate that the transition excited at 266 nm is the $S_0 \rightarrow S_2$ transition since the calculated vertical excited energy to S2 is quite close to the photon energy. Moreover, the oscillator strength of S_2 is 70 times greater than that of S_1. This confirms that the initial excitation of the C_6H_5NO photodissociation at 266 nm is a $S_0 \rightarrow S_2$ transition. With the analysis of the orbital coefficient of excited states, the excited singlet states (S_1 and S_2) might be regarded as ($\pi-\pi^*$) transitions. However, the first singlet state was attributed mainly to the excitation of an electron among N and O atoms and of the C atom which links to N; the second excited singlet state (S_2) was attributed to the excitation of the benzene ring, with little contribution from the N and O orbitals. On the basis of the analysis above, we qualitatively proposed the possible photodissociation mechanism. It is more probable that the laser will promote vertically the wave packet to the S_2 state of nitrosobenzene; then the predissociation will take place via intramolecular vibrational energy redistribution or nonradiative electronic relaxation from the initial S_2 excited state to the lower triplet state or the singlet state. An alternative mechanism is that the dissociation might occurthrough the intersystem crossing from the initial excited-state S_2 to the upper electronic repulsive triplet state as well. It should be noted that ab initio results are rather crude due to the calculations performed at the lower level. Thus, further experimental and theoretical work is being carried out to interpret the photodissociation mechanism of this molecule more clearly.

5. Conclusion

By the technique of photofragment translational spectroscopy, we have first studied the photodissociation dynamics of nitrosobenzene at 266 nm under collision-free conditions. Angle-resolved NO and C_6H_5 TOF spectra from C_6H_5NO photodissociation are measured, and the photofragment translational energy distribution is determined. The photofragment translational energy distribution $P(E_t)$ reveals that about 29% of the available energy is partitioned into translational energy and about 71% into internal excitation of the phenyl radical and NO products. The anisotropy parameter β at this wavelength is determined to be −0.64. The perpendicular transition dominates over the parallel transition in C_6H_5NO photodissociation. The geometries of the ground state, the singlet excited states, and the triplet excited states are optimized, and the probable photodissociation mechanism is suggested.

Acknowledgment. The authors thank Prof. Yuan Tseh Lee, Prof. Xinsheng Zhao, and Prof. Xueming Yang for supplying the CMLAB2 program and giving helpful advice. This work is supported by Outstanding Young Scientist Awards of National Natural Science Foundation of China, the State Committee of Science and Technology of China (No. 29825107).

References and Notes

(1) Simons, J. P. *J. Phys. Chem.* **1984**, *88*, 1287.
(2) Shapiro, M.; Bersohn, R. *Annu. Rev. Phys. Chem.* **1982**, *33*, 409.
(3) Busch, G. E.; Cornelius, J. F.; Mahoney, R. T.; Morse, R. I.; Schlosser, D. W.; Wilson, K. R. *Rev. Sci. Instrum.* **1970**, *41*, 1066.
(4) Busch, G. E.; Wilson, K. R. *J. Chem. Phys.* **1972**, *56*, 3626, 3638, 3655.
(5) Ashfold, M. N. R.; Lambert, I. R.; Mordaunt, D. H.; Morley, G. P.; Western, C. M. *J. Phys. Chem.* **1992**, *96*, 2938.
(6) Minton, T. K.; Nelson, C. M.; Moore, T. A.; Okumura, M. *Science* **1992**, *258*, 1342.
(7) Butler, L. J.; Neumark, D. M. *J. Phys. Chem.* **1996**, *100*, 12801.
(8) Wang, G. J.; Zhu, R. S.; Zhang, H.; Han, K. L.; He, G. Z.; Lou, N. Q. *Chem. Phys. Lett.* **1998**, *288*, 429.
(9) Zhang, H.; Zhu, R. S.; Wang, G. J.; Han, K. L.; He, G. Z.; Lou, N. Q. *J. Chem. Phys.* **1999**, *110*, 2922.
(10) Wang, G. J.; Zhang, H.; Zhu, R. S.; Han, K. L.; He, G. Z.; Lou, N. Q. *Chem. Phys.* **1999**, *241*, 213.
(11) Zhu, R. S.; Zhang, H.; Wang, G. J.; Han, K. L.; He, G. Z.; Lou, N. Q. *Chem. Phys. Lett.* **1999**, *313*, 98.
(12) Zhang, H.; Zhu, R. S.; Wang, G. J.; Han, K. L.; He, G. Z.; Lou, N. Q. *Chem. Phys. Lett.* **1999**, *300*, 483.
(13) Zhu, R. S.; Zhang, H.; Wang, G. J.; Han, K. L.; He, G. Z.; Lou, N. Q. *Chem. Phys.* **1999**, *248*, 285.
(14) Yang, S.; Bersohn, R. *J. Chem. Phys.* **1974**, *61*, 4400.
(15) Dzvonik, R.; Yang, S.; Bersohn, R. *J. Chem. Phys.* **1974**, *61*, 4408.
(16) Kawasaki, M.; Lee, S. J.; Bersohn, R. *J. Chem. Phys.* **1977**, *66*, 2647.
(17) Freedman, A.; Yang, S. C.; Wawasaki, M.; Bersohn, R. *J. Chem. Phys.* **1980**, *72*, 1028.
(18) Ichimura, T.; Mori, Y.; Shinohara, H.; Nishi, N. *Chem. Phys. Lett.* **1985**, *122*, 51.
(19) Ichimura, T.; Mori, Y.; Shinohara, H.; Nishi, N. *Chem. Phys. Lett.* **1985**, *122*, 55.
(20) Ichimura, T.; Mori, Y.; Shinohara, H.; Nishi, N. *Chem. Phys.* **1994**, *189*, 117.
(21) Ichimura, T.; Mori, Y.; Shinohara, H.; Nishi, N. *J. Chem. Phys.* **1997**, *107*, 835.
(22) Hwang, H. J.; EI-Sayed, M. A. *J. Chem. Phys.* **1992**, *96*, 856.
(23) Okabe, H. In *Photochemistry of Small Molecules*; Wiley-Interscience: New York, 1978.

(24) Kawasaki, M.; Kasatani, K.; Sato, H.; Shinohara, H.; Nishi, N. *Chem. Phys.* **1984**, *88*, 135.
(25) van Veen, G. N. A.; Baller, T.; de Vries, A. E. *Chem. Phys.* **1985**, *92*, 59.
(26) Sparks, R. K.; Shobatake, K.; Carlson, L. R.; Lee, Y. T. *J. Chem. Phys.* **1981**, *75*, 3838.
(27) Continetti, R. E.; Balko, B. A.; Lee, Y. T. *J. Chem. Phys.* **1988**, *89*, 3383.
(28) Barry, M. D.; Gorry, P. A. *Mol. Phys.* **1984**, *52*, 461.
(29) Butler, L. J.; Hintsa, E. J.; Lee, Y. T. *J. Chem. Phys.* **1986**, *84*, 4104.
(30) Butler, L. J.; Hintsa, E. J.; Shane, S. F.; Lee, Y. T. *J. Chem. Phys.* **1987**, *86*, 2051.
(31) Nadler, I.; Reisler, H.; Noble, M.; Wittig, C. *Chem. Phys. Lett.* **1984**, *108*, 115.
(32) Knee, J. L.; Khumdkar, L. R.; Zewail, A. H. *J. Chem. Phys.* **1985**, *89*, 4659.
(33) Qian, C. X. M., et al. *J. Chem. Phys.* **1985**, *83*, 5573.
(34) Noble, M.; Qian, C. X. M.; Reisler, H.; Wittig, C. *J. Chem. Phys.* **1986**, *85*, 5763.
(35) Reisler, H.; Pessine, F. B. T.; Haas, Y.; Wittig, C. *J. Chem. Phys.* **1983**, *78*, 3785.
(36) Dixon, R. N.; Jones, K. B.; Noble, M.; Carter, S. *Mol. Phys.* **1981**, *42*, 455.
(37) Bower, R. D.; Jones, R. W.; Houston, P. L. *J. Chem. Phys.* **1983**, *79*, 2799.
(38) Dekoven, B. M., et al. *J. Chem. Phys.* **1981**, *74*, 4755.
(39) Spears, K. G.; Hoffland, L. D. *J. Chem. Phys.* **1981**, *74*, 4765.
(40) Roellig, M. P.; Houston, P. L. *Chem. Phys. Lett.* **1975**, *57*, 75.
(41) Roellig, M. P.; Houston, P. L.; Asscher, M.; Haas, Y. *J. Chem. Phys.* **1980**, *73*, 5081.
(42) Jones, R. W.; Bower, R. D.; Houston, P. L. *J. Chem. Phys.* **1982**, *76*, 3339.
(43) Dyet, J. A.; McCoustra, M. R. S.; Pfab, J. *J. Chem. Soc., Faraday Trans. 2* **1988**, *84*, 463.
(44) Spasov, J. S.; Cline, J. I. *J. Chem. Phys.* **1999**, *110*, 9568.
(45) McCoustra, M. R. S.; Dyet, J. A.; Pfab, J. *Chem. Phys. Lett.* **1987**, *136*, 231.
(46) Nakamoto, K.; Rundle, R. E. *J. Am. Chem. Soc.* **1956**, *78*, 1113.
(47) Labhart, H.; Wagniere, G. *Helv. Chim. Acta* **1963**, *46*, 1314.
(48) Tabei, K.; Nagakura, S. *Bull. Chem. Soc. Jpn.* **1965**, *38*, 965.
(49) Wodtke, A. M.; Hinsta, E. J.; Lee, Y. T. *J. Phys. Chem.* **1986**, *90*, 3549.
(50) Tsang, W.; Robaugh, D.; Mallard, W. *J. Phys. Chem.* **1986**, *90*, 5968.
(51) Blais, N. C. *J. Chem. Phys*. **1983**, *79*, 708.
(52) Kwok, H. S.; He, G. Z.; Sparks, R. K.; Lee, Y. T. *Int. J. Chem. Kinet.* **1981**, *13*, 1125.
(53) Turnipseed, A. A.; Vaghjiani, G. L.; Thompson, J. E.; Ravishankara, A. R. *J. Chem. Phys.* **1992**, *96*, 5887.
(54) Galloway, D. B.; Barts, J. A.; Huey, L. G.; Crim, F. F. *J. Chem. Phys.* **1993**, *98*, 2107.
(55) Choo, K. L.; Golden, D. M.; Benson, S. W. *Int. J. Chem. Kinet.* **1975**, *7*, 713.
(56) Park, J.; Dyakov, I. V.; Mobel, A. M.; Lin, M. C.; *J. Phys. Chem. A* **1997**, *101*, 6043.
(57) Qi, J. X. Ph.D. Thesis, Dalian Institute of Chemical Physics, Chinese Academy of Sciences, Dalian, 1993.
(58) Qi, J. X.; Wang, G. J.; Han, K. L.; Sha, Y. X.; He, G. Z.; Lou, N. Q. *Mol. Phys.* **1997**, *92*, 71.
(59) Vernon, M. *KELVIN Rare Gas Time-of-Flight Program*; Lawrence Berkeley Laboratory Report No. 12422; Lawrence Berkeley Laboratory: Berkeley, CA, 1981.
(60) Krajnovich, D. J. Ph.D. Thesis, University of California, Berkeley, CA, 1983.
(61) Hintsa, E. J.; Zhao, X.; Lee, Y. T. *J. Chem. Phys.* **1990**, *92*, 2280.
(62) Zhao, X. Ph.D. Thesis, University of California, Berkeley, CA 1988.
(63) Zare, R. N. *Mol. Photochem.* **1972**, *4*, 1.
(64) Dubs, M.; Huber, J. R. *Chem. Phys. Lett.* **1984**, *108*, 123.
(65) Lahmani, F.; Lardeux, C.; Solgadi, D. *Chem. Phys. Lett.* **1983**, *102*, 523.
(66) Pfab, J.; Hager, J.; Krieger, W. *J. Chem. Phys.* **1983**, *78*, 266.
(67) Pak, K.; Testa, A. C. *J. Phys. Chem.* **1972**, *76*, 1087.
(68) Frisch, M. J., et al. *GAUSSIAN 94 (Revision A)*; Gaussian, Inc.: Pittsburgh, PA, 1995.
(69) Foresman, J. B.; Head-Gordon, M.; Pople, J. A. *J. Phys. Chem.* **1992**, *96*, 135.
(70) Schlegel, H. B.; Foresman, J. B. *NATO-ASI Series C*; Kluwer Academic: Dordrecht, The Netherlands, 1993; pp 11−20.